Possible role of amphibole in the origin of andesite: some experimental and natural evidence

Article *in* Contributions to Mineralogy and Petrology · February 1992

DOI: 10.1007/BF00306551

2 authors:

John Foden
University of Adelaide
176 PUBLICATIONS **6,363** CITATIONS

SEE PROFILE

David Headley Green
University of Tasmania
268 PUBLICATIONS **27,145** CITATIONS

SEE PROFILE

Contrib Mineral Petrol (1992) 109:479–493

Contributions to Mineralogy and Petrology

Possible role of amphibole in the origin of andesite: some experimental and natural evidence

J.D. Foden[1] and D.H. Green[2]

[1] Department of Geology and Geophysics, University of Adelaide, Box 498 G.P.O., Adelaide, South Australia, Australia
[2] Department of Geology, University of Tasmania, Box 252c, G.P.O., Hobart, Tasmania, 7001, Australia

Received June 19, 1989/Accepted June 17, 1991

Abstract. Experiments in the system high-Al basalt (HAB)-water have been conducted in the melting range at pressures between 1 atm. and 10 kbar, defining the amphibole stability field and the composition of liquids which coexist with this amphibole. Plagioclase is the anhydrous liquidus phase between 1 atm. and 10 kbar but in the hydrous runs this role is taken by olivine at <7 kbar and then by clinopyroxene at higher pressures. Because amphibole is never on the high-Al basalt liquidus it is not likely that andesite is derived from primary basalt by pure fractional crystallisation, although as we discuss, other mechanisms including equilibrium crystallisation might implicate amphibole. If primary basaltic magma undergoes closed-system equilibrium crystallisation, then the amphibole field will be intersected at between 50 and 100 °C below the liquidus. The compositions of melts coexisting with amphibole alone do not match those of any of the natural andesite or dacitic lavas associated with the particular high-Al basalt investigated. Like natural andesites, they become rapidly silica enriched, but they also become far more depleted in TiO_2 and MgO. However, the compositions of liquids lying directly on the divariant amphibole-out reaction zone, where amphibole + liquid coexist with clinopyroxene or olivine ($\pm$ plagioclase), do resemble those of naturally occurring low-silica andesites. With increasing temperature pargasitic amphibole breaks down via incongruent melting reactions over a narrow temperature range to form a large volume of relatively low-silica basaltic andesite liquid and a crystalline assemblage dominated by either clinopyroxene or olivine. Our important conclusion is that basaltic andesite liquid will be the product of reaction between cooling, hydrous mafic liquid and anhydrous ferromagnesian phases. The solid reactants could represent earlier cumulates from the same or different magma batches, or they could be peridotite wall-rock material. Because the amphibole-out boundary coexisting with liquid is one of reaction, it will not be traversed so long as the phases on the high temperature side remain. Thus, the assemblage amphibole + clinopyroxene $\pm$ olivine $\pm$ plagioclase + liquid is one in which the liquid is buffered (within limits), and results reported here indicate that this buffering generates melts of low-silica andesite composition. When tapped to lower pressures these liquids will rise, eventually to fractionate plagioclase-rich assemblages yielding silica-rich andesite and dacite melts. Conversely, the partial melting of hornblende pyroxenite, hornblende peridotite or hornblende gabbro can also yield basaltic andesite liquids. The phase relationships suggested by these experiments are discussed in the light of naturally occurring phenocryst and xenolith assemblages from the east Sunda Arc. Primary magmatic additions to the lithosphere of volcanic arcs are basaltic and voluminous upper crustal andesite in these terranes, complemented by mafic and ultramafic crystalline deposits emplaced in the lower crust or close to the Moho. Together these components constitute total arc growth with a basaltic composition and represent the net accreted contribution to continental growth.

Introduction

Given the potential role of arc accretion and hence of island arc magmatism to continental crustal growth (e.g. Taylor and McLennan 1985), the origin of andesite is an important problem which has created extensive debate (Gill 1981). In this paper we present evidence which supports a common although not universal opinion amongst petrologists (Foden 1983; Crawford et al. 1987), that andesite is a differentiate of parental basaltic magmas. This paper develops and discusses the concept that the primary magmatic additions to the arc lithosphere are basaltic and that voluminous upper crustal andesite is complemented by mafic and ultramafic crystalline deposits emplaced in the lower crust or the upper lithospheric mantle. Together these components constitue whole-arc lithosphere growth. However, because the petrogenetic processes we discuss in this paper create this separation into upper crustal andesite and lower crustal or upper mantle pyroxenitic and

Offprint requests to: J.D. Foden

amphibolitic components, the geochemical impact of continental crust growth by marginal accretion will depend very much on whether such accretion is of the whole lithosphere or just the crust.

One central issue is to determine those components of the geochemical signature of arc magmas which are dictated by *process* and those which reflect separate *source components* of distinctive composition. Although their trace elements characteristics implicate the role of other source reservoirs, the broad implication of Nd isotopic data published on many island arcs in the past decade is that a substantial proportion of most arc magma has an origin in the contemporary depleted mantle wedge. Yet when compared with the other major sites of mantle-derived terrestrial magmatism, principally the mid ocean ridges, ocean islands and continental break-up zones, arcs are dominated by significantly more siliceous rocks (andesites and dacites) which occur together with basalts. Andesite may originate as a derivative of mantle melting by virtue of a process unique to the arc environment, or it may be the result of unique or unusual combination of source material compositions.

Several mechanisms have been put forward to account for the occurrence and composition of andesite. These include direct melting of the upper portion of the subducted slab, a primary origin by melting of a hydrated peridotite component of the mantle wedge, and various fractioanal crystallisation mechanisms involving basaltic primary magmas which are themselves the product of fusion of the hydrated peridotite (e.g. Ringwood 1974).

Volcanological and petrographic characteristics of island arc magmatism show that water plays a key role. These include common explosive volcanic eruptions, the development of highly vesicular magmatic products (pumice flows etc.), eruption of phenocryst-rich magmas with dramatic zonation of phenocrysts, and the frequent preservation of hydrous mineral phases.

Even though it is well established that the presence of water in peridotite systems extends the incongruent melting behaviour of enstatite to quite high pressures, thereby expanding the stability field of liquidus olivine to relatively silicic compositions (e.g. Kushiro 1972; Nicholls and Ringwood 1973; Nicholls 1974; Green 1976), it is not likely that island arc andesites represent liquids in equilibrium with mantle olivine. They are typically fractionated rocks with low Ni contents and Mg/(Mg + Fe) values inappropriate for primary mantle melts (e.g. Crawford et al. 1987).

If andesites are not primary magmas but are in fact fractionated liquids, then which phases control the line of liquid descent? Gill (1981) suggests that the most important influence is that of the combined crystallisation of plagioclase + augite + olivine + magnetite (POAM) from parental basalt magma, but a considerable number of studies (e.g. Cawthorn 1976; Cawthorn and O'Hara 1976; Green 1982; Foden 1983) suggest that amphibole plays an influential role, at least in some arc magmatic systems. Because of the very low SiO_2 content of pargasitic amphibole (<40% SiO_2) its crystallisation will promote efficient silica enrichment of derivative liquids (e.g. Foden 1983).

This paper presents new experimental data in the system high-alumina basalt (HAB) + water at pressures between 1 atmosphere and 10 kbar which allow this problem to be more precisely assessed. The models based on these experimental data are examined in the light of petrological information from volcanic rocks and mafic to ultramafic xenoliths from island arcs.

Experimental methods and calculation of the equilibrium liquid compositions

Experiments were all conducted at the University of Tasmania. Those at elevated pressure were made using Boyd-England type piston-cylinder equipment, while sealed and evacuated silica glass tubes were used in runs at <1 atmosphere. The runs at elevated pressures used combinations of talc, Pyrex glass, NaCl and boron nitride components as run assemblages and pressure media. The starting material (Table 1) was composed of finely ground glass prepared from a mafic high-Al basalt from Rindjani volcano from the eastern Sunda Arc (Foden 1983). This was welded into Ag–Pd capsules with weighed quantities of water.

The major objectives of the experimental program were to determine the phase relations in the system natural HAB + H_2O, within 250 °C of the liquidus at pressures up to 10 kbar and particularly to determine the composition of the equilibrium liquids on either side of the amphibole-out boundary. The phase relations are presented in Figs. 1 and 2, and the details of the experimental run products are summarised in Table 2. Recalculated compositions of the experimental liquids are given in Table 3, and the compositions of synthesised amphiboles are given in Table 4.

Considerable care was taken in the treatment of the glass analyses to ensure as far as possible that these represented equilibrium melts. There are three main sources of discrepancy between direct electron microprobe analyses of glass and true compositions of the equilibrium liquids. These factors are iron-loss to the Ag–Pd capsule, modification of liquids during rapid disequilibrium crystal growth on quenching of the run, and Na-volatilisation from H_2O-bearing glasses during analysis with the electron probe. Iron loss is most serious in those runs conducted at highest temperatures and seemed to have only a minor impact on most of these experiments. It results from the alloying of Fe from the melt in its reduced state with the capsule metal. Fe reduction in turn is promoted by reaction with hydrogen formed by the hydrolysis of the hydroxyl component from the talc sleeve which is diffused through the capsule wall.

In order to limit Fe-loss, run times were as short as possible consistent with the establishment of equilibrium. The growth of equilibrium phases was promoted by the use of the crystal-free starting material (finely ground glass) and by heating the run up to the appropriate temperature. As the approach to the run condition

Table 1. Analyses of experimental starting material, basalt 41632, and representative basaltic andesite, andesite and dacite from Rindjani (1) volcano

Sample No.	41632 B	41637 BA	41625 A	41636 A	41671 D
SiO_2	49.77	52.97	56.18	58.91	65.58
TiO_2	1.13	0.96	0.88	0.7	0.65
Al_2O_3	17.84	19.35	18.37	18.41	16.65
FeO	9.75	9.13	7.54	6.89	3.86
MnO	0.15	0.18	0.17	0.17	0.13
MgO	6.49	2.91	3.54	2.32	1.12
CaO	10.45	8.47	7.55	7.09	3.09
Na_2O	3.04	4.05	3.86	3.77	4.95
K_2O	1.20	1.69	1.61	1.37	3.67
P_2O_5	0.18	0.24	0.25	0.22	0.22

1. Note: Rindjani Volcano, see Foden 1983.
B = high-Al basalt, BA = basaltic andesite, A = andesite and D = dacite

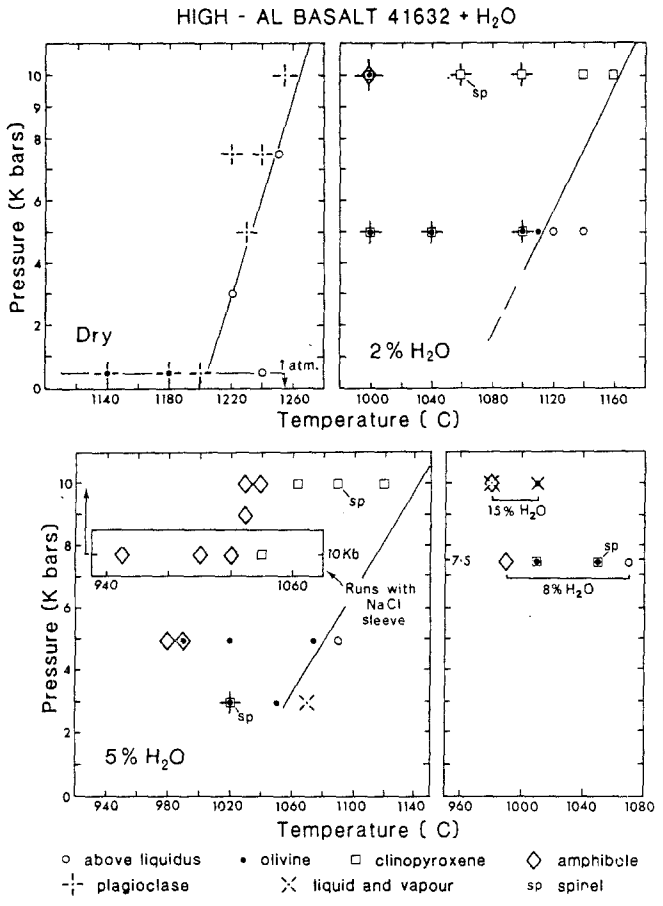

Fig. 1. Summary of the results of experiments in the system high-Al basalt-H_2O. The position of the liquidus is indicated in the diagrams representing dry, 2% and 5% water results. Run conditions and products are listed in Table 2

was thus prograde, excess activation energy was thereby provided continuously to re-equilibrate lower temperature nuclei while care was taken not to overshoot run temperatures to prevent the preservation of metastable (high temperature) nuclei. Some lower temperature runs which contained high percentages of crystals required more lengthy equilibration times. These were made in Ag75 Pd25 capsules which together with the adoption of anhydrous NaCl sleeves in place of talc (eliminating the source of hydrogen) largely preventing iron loss.

The effects of sodium volatilisation during microprobe analysis are illustrated in Fig. 3 and are a function of the degree of hydration of the glass. Note that in Fig. 3, SiO_2 concentration is a function of fraction of crystallisation, which is turn results in enrichment of the H_2O content of the melt. These analyses were made with defocussed electron beams of either 10 or 20 μm diameter. If very large pools of glass were available, analyses were also made using beam rastering. In spite of these precautions those runs like T1383 (Table 3), whose proportion of crystals exceeds 50%, have residual liquids with ~ 10 wt. %H_2O and the microprobe analyses of the these register less than 30% of the true Na_2O content of the glass.

In reconstructing the melt composition indirectly represented by our glass analyses, a mass balance was established using least squares mixing techniques. As illustrated by the example given in Table 5, the bulk starting composition and the compositions of the analysed minerals were combined to yield a best approximation of the microprobe analysis of the glass composition. This approximation is totally consistent with the mass balance requirements and became the estimated glass composition taken to represent our melt. The calculations also give us the relative proportions of the minerals as well as the total fraction of crystallisation. These estimates of proportions were consistent with point counting SEM photographs of run fragments undertaken on selected charges. They also yielded smooth variations in composition and crystal content between different isobaric runs, of common bulk composition, as a function of temperature. Because the method of recalculation restores the Fe-loss it introduces a small error. Equilibria were in reality established over the period of the run, and partial restoration of the iron would be most appropriate. The minor Fe-loss experienced by these experiments has the effect of shifting ferromagnesian phase boundaries to slightly higher temperatures, but does not influence the general form of the diagrams or our conclusions.

It should be noted that where runs intially performed using talc sleeves have been repeated in NaCl, products of the latter are often slightly less crystalline at any given temperature because their bulk Mg# $\left(\text{Mg\#} = \frac{\text{Mg}}{\text{Mg} + \Sigma\text{Fe}} \text{mols.} \right)$ values have not been raised by iron-loss. The Fe-loss resulting from a run of 1 hour duration at about 1050 °C in an assemblage with talc has the capacity to displace phase boundaries as much as 10–20°C up-temperature. If this phase boundary is a reaction curve which consumes large volumes of melt, then two runs which straddle it will yield quite different liquid proportions and compositions. For this reason there is sometimes some disparity between NaCl and talc runs nominally made at the same conditions (runs T933 and T1377; Tables 2 and 3).

The starting material used in the experiments (Table 1) is a natural high-Al basalt from Rindjani volcano on the island of Lombok, Indonesia. This volcano has been extensively studied (Foden and Varne 1980; Foden 1983; Varne and Foden 1986) and has erupted a diverse range of calc-alkaline lavas ranging from high-Al basalts through andesite to dacite. Foden (1983) interpreted the relatively low K_2O content of the andesites when compared with those of coeval basalts as indicative of the influence of amphibole crystallisation. Although the mineralogy of these lavas is dominated by pyroxenes, plagioclase, magnetite and olivine, some reacted relicts of pargasitic amphibole are occasionally recognised. It was also demonstrated that the plagioclase-rich phenocryst assemblages of the highly porphyritic andesites were largely in equilibrium with siliceous dacitic liquids and did *not* represent assemblages responsible for the evolution of andesite liquid from basalt. The trends defined by the Rindjani andesites and dacites offer a natural yardstick against which the experimentally synthesised liquids can be compared.

Experimental results

Phase relations

At 1 atm. and at higher pressures with very low water content (< 2.0%) the liquidus phase is plagioclase (Fig. 1). With greater amounts of water the liquidus phase is either olivine or clinopyroxene, the upper pressure limit of liquidus olivine increasing from > 5 kbar with 2% H_2O to > 10 kbar water saturated (cf. Nicholls and Ringwood 1973). The plagioclase field shows the well established (e.g. Yoder and Tilley 1962) contraction to lower temperatures at increased H_2O content at 5 and 10 kbar.

Amphibole does not occur on this basaltic liquidus; its appearance is always preceded at higher temperatures by clinopyroxene and/or olivine, and at low water contents, sometimes by plagioclase (Fig. 2). The amphibole-out curve shows a thermal maximum as a function of wt.% H_2O which shifts slightly towards lower concentrations of water with increasing pressure (Fig. 2). This is in accordance with the findings of Eggler (1972), Holloway and Burnham (1972), Eggler (1973) and Holloway (1973).

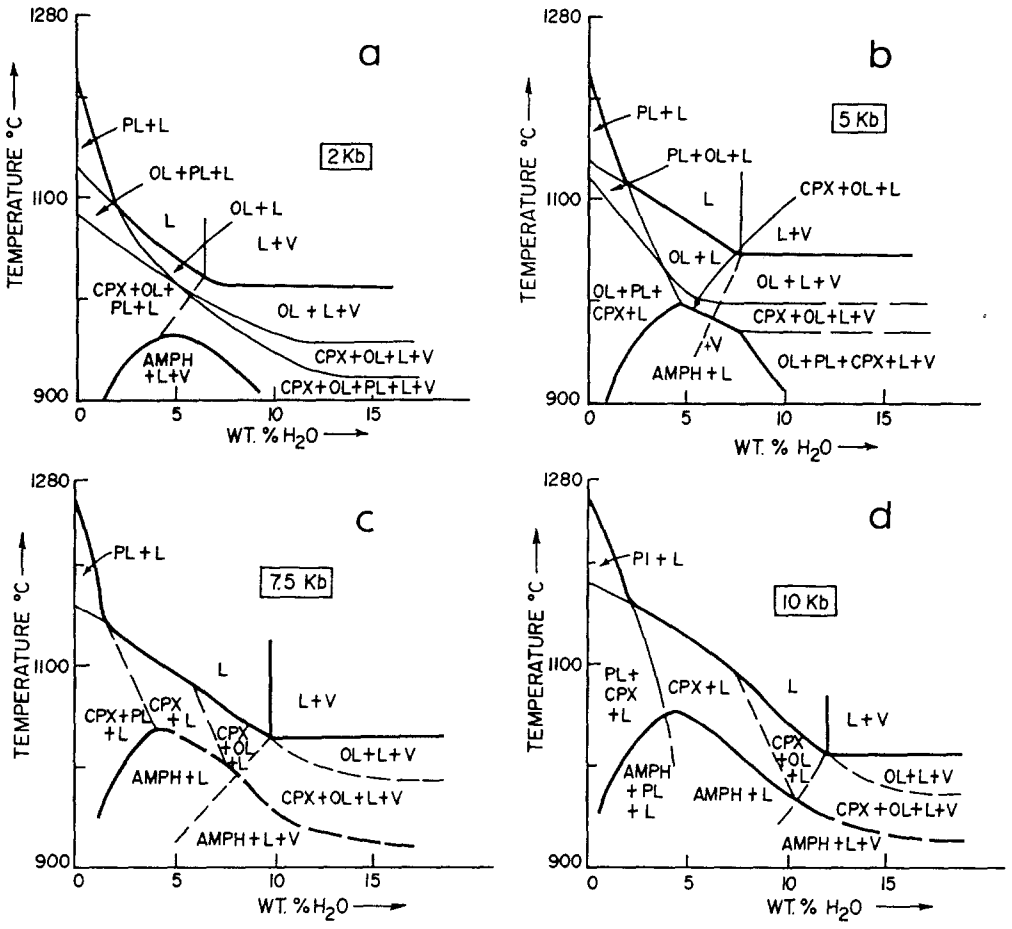

Fig. 2a–d. Summary isobaric T-wt% H_2O sections in the system HAB 41632-H_2O at various pressures. Water quoted as total percentage of the system. The amount of crystallisation in specific runs and calculated H_2O content of the liquid are given in Table 3

The nature of the isobaric amphibole-breakdown reaction with heating varies as a function of pressure and $\%H_2O$. At low pressures ($< \sim 2$ kbar) amphibole breaks down to an assemblage $ol + cpx + pl + L \pm V$. At intermediate pressures (~ 5 kbar) the breakdown products are olivine or olivine and clinopyroxene, and at higher pressures (~ 10 kbar) clinopyroxene is formed. As discussed by Cawthorn (1976) and Cawthorn and O'Hara (1976), the reactions to produce olivine or clinopyroxene are incongruent at the pressures considered here. Both olivine and clinopyroxene thus appear to be in a reaction relationship with the liquid and are eliminated at, or very close to, the amphibole-out curve in the pressure range studied. The approximate stoichiometry of this reaction at 10 kbar with 5% H_2O (Fig. 2d) is (by weight):

100 *Amphibole* = 35 *Cpx* + 65 *Liquid.*

This stoichiometry, calculated from the variation in mineral and liquid proportions as a function of temperature derived from the mass balance calculations (e.g. Table 5), represents the end results of the completed reaction. Naturally the compositions of the amphibole and clinopyroxene will change *during* the reaction, which will occupy a divariant field and take place over some finite temperature interval (< 20°C). This relationship is indicated in Fig. 5 where the liquid composition occupies an interval on the reaction boundary, amphibole + Liquid ↔ clinopyroxene + Liquid.

The important implications are that large quantities of melt are consumed when amphibole becomes stable on cooling, or that in case of vapour-absent melting of amphibolite large amounts of liquid are produced isothermally. If, as in the case of these experiments, the composition of the bulk system is such that the amphibole stability field is within the melting range, then the reaction at 10 kbar could be described thus:

Liquid 2 + *Amphibole* = *Cpx* + *Liquid* 1.

As these amphiboles are very subsilicic (Table 4), with 40–42 wt.% SiO_2 compared with clinopyroxene (50–52 wt.% SiO_2), Liquid 2 on the low temperature side of the reaction is much richer in SiO_2 than Liquid 1 on the high temperature side.

From the isobaric sections (Fig. 2) it can be seen that the precise form of the amphibole melting reaction changes as a function of pressure, temperature and water content. It should be emphasised that the reaction described above is an example of one of a number of specific stoichiometries that will vary according to the pressure and the bulk composition of the system. For instance, in a system of HAB bulk composition, the simple amphibole-out reaction illustrated above is restricted to pressures

Table 2. Experimental conditons and results

Run No.	Temp. °C	Pressure kbar	% H_2O	Duration Hrs	Capsule	Run assembly	Phases
AT107	1240	1 atm.	0	0.5	Fe	SiO_2 Tube	L
AT104	1200	1 atm.	0	1	Fe	SiO_2 Tube	L, PI
AT106	1180	1 atm	0	1.5	Fe	SiO_2 Tube	L, PI, OI
AT105	1140	1 atm.	0	1.5	Fe	SiO_2 Tube	L, PI, OI
T1090	1220	3	0	1	Fe	Talc/Pyrex/BN	L
T173	1070	3	5	0.5	Ag50 Pd50	Talc/BN	L, V
T174	1050	3	5	0.5	Ag50 Pd50	Talc/BN	L, OI, V
T177	1020	3	5	0.5	Ag50 Pd50	Talc/BN	L, OI, CPX, SP
T1089	1230	5	0	1	Fe	Talc/Pyrex/BN	L, PI
T75	1140	5	2	0.5	Ag50 Pd50	Talc/BN	L
T76	1120	5	2	0.5	Ag50 Pd50	Talc/BN	L
T78	1110	5	2	0.5	Ag50 Pd50	Talc/BN	L, OI
T70	1100	5	2	0.5	Ag50 Pd50	Talc/BN	L, OI, CPX, PI
T71	1040	5	2	0.5	Ag75 Pd25	Talc/BN	L, OI, CPX, PI
T82	1000	5	2	0.7	Ag75 Pd25	Talc/BN	L, OI, CPX, PI, AMP
T125	1090	5	5	0.5	Ag50 Pd50	Talc/BN	L
T127	1075	5	5	0.5	Ag50 Pd50	Talc/BN	L, OI
T131	1020	5	5	0.5	Ag50 Pd50	Talc/BN	L, OI
T151	990	5	5	0.5	Ag50 Pd50	Talc/BN	L, OI, AMP
T150	980	5	5	0.5	Ag50 Pd50	Talc/BN	L, AMP
T991	1250	7.5	0	1	Graphite	Talc/Pyrex/BN	L
T1085	1240	7.5	0	1	Graphite	Talc/Pyrex/BN	L, PI
T1084	1220	7.5	0	1	Graphite	Talc/Pyrex/BN	L, PI
T172	1070	7.5	8	0.5	Ag50 Pd50	Talc/BN	L
T170	1050	7.5	8	0.5	Ag50 Pd50	Talc/BN	L, OI, CPX, SP
T990	1010	7.5	8	1	Ag50 Pd50	Talc/BN	L, OI, CPX
T1000	990	7.5	8	1	Ag50 Pd50	Talc/BN	L, AMP
T994	1030	9	5	1	Ag50 Pd50	Talc/BN	L, AMP
T992	1260	10	0	1	Graphite	Talc/Pyrex/BN	L
T1086	1255	10	0	1	Graphite	Talc/Pyrex/BN	L, PI
T87	1167	10	2	0.5	Ag50 Pd50	Talc/BN	L, CPX
T86	1140	10	2	0.5	Ag50 Pd50	Talc/BN	L, CPX
T83	1100	10	2	0.5	Ag50 Pd50	Talc/BN	L, CPX
T84	1060	10	2	0.5	Ag50 Pd50	Talc/BN	L, CPX, SP
T85	1000	10	2	0.7	Ag50 Pd50	Talc/BN	L, CPX, PI, AMP, SP
T1498	1000	10	2	22.5	Ag75 Pd25	NaCl/BN	L, OI, PI, AMP
T989	1120	10	5	1	Ag50 Pd50	Talc/BN	L, CPX
T153	1090	10	5	0.5	Ag50 Pd50	Talc/BN	L, CPX, SP
T175	1065	10	5	0.5	Ag50 Pd50	Talc/BN	L, CPX
T993	1040	10	5	1	Ag50 Pd50	Talc/BN	L, AMP
T1377	1040	10	5	6	Ag75 Pd25	NaCl/Pyrex/BN	L, CPX
T159	1030	10	5	0.5	Ag50 Pd50	Talc/BN	L, AMP
T1384	1020	10	5	6	Ag75 Pd25	NaCl/Pyrex/BN	L, AMP
T1091	1010	10	15	1	Ag75 Pd25	Talc/BN	L, OI, V
T1379	1000	10	5	6	Ag75 Pd25	NaCl/Pyrex/BN	L, AMP
T1088	980	10	15	1	Ag75 Pd25	Talc/BN	L, AMP, V
T1383	950	10	5	19	Ag75 Pd25	NaCl/BN	L, AMP

> 6 kbar in an area of T–H_2O space which expands with increasing P. Clearly the compositions of liquids formed as a result of these breakdown reactions must also vary in detail.

Taking the 10 kbar section as an example, liquid immediately on the high T side of the amphibole-out curve will become more silica-rich as the water content of the system increases. This is because the net silica content of the breakdown products decreases as they change progressively from clinopyroxene to clinopyroxene + olivine.

For water undersaturated conditions the dP/dT slope of the amphibole-out curves is likely to remain positive to pressures of the order of 20–25 kbar at which stage amphibole is eliminated by reactions producing garnet (e.g. Allen and Boettcher 1978). In our experiments, we did not directly control f_{O_2}. This is buffered by the furnace assemblage and experiments conducted with companion capsules containing ilmenite-magnetite mixtures reveal f_{O_2} conditions close to the wüstite-magnetite buffer. The results of Helz (1982) suggest that, when conditions are more oxidising than the NNO buffer, increased f_{O_2} may result in slightly decreased upper stability temperatures for hornblende although the trends are not clear. The conditions in these runs are probably more reduced than those in island arc magma systems (andesites are possibly about one log unit above NNO according to Gill 1981) with the possible

Table 3. Recalculated compositions of melts from experimental runs

Run Number	AT104	AT106	AT105	T78	T70	T71	T82*	T127	T131
Temperature °C	1200	1180	1140	1110	1100	1040	1000	1075	1020
Pressure kbar	1 atm	1 atm	1 atm	5 atm	5 atm	5 atm	5 atm	5 atm	5 atm
$\%H_2O$	0	0	0	2	2	2	2	5	5
SiO_2	49.64	50.21	50.12	49.81	49.77	50.18	51.02	49.72	50.09
TiO_2	1.16	1.40	1.54	1.14	1.16	1.41	1.62	1.13	1.16
Al_2O_3	17.39	16.55	15.22	17.91	18.71	20.07	18.91	17.85	18.37
Fe_2O_3		0.45		1.60	1.55	3.90	3.98	0.51	0.91
FeO	9.97	10.35	10.86	8.29	8.58	6.99	6.76	9.26	8.64
MnO	0.15	0.17	0.16	0.15	0.15	0.16	0.16	0.15	0.15
MgO	6.63	5.88	5.05	6.34	5.68	3.35	2.31	6.41	5.46
CaO	10.24	10.18	9.13	10.50	9.77	9.06	9.48	10.46	10.76
Na_2O	3.06	3.24	3.79	3.05	3.27	3.91	3.98	3.04	3.13
K_2O	1.22	1.43	1.58	1.21	1.30	1.69	1.88	1.20	1.23
P_2O_5	0.18	0.22	0.23	0.18	0.20	0.26	0.30	0.18	0.19
Mg/Mg+Fe	0.54	0.50	0.45	0.58	0.54	0.46	0.38	0.55	0.53
K_2O/Na_2O	0.40	0.44	0.42	0.40	0.40	0.43	0.47	0.39	0.39
wt % Crystallisation	2.80	19.30	27.50	0.50	9.00	29.42	58.00	0.20	3.00
wt % H_2O in liquid	0.00	0.00	0.00	2.01	2.20	2.85	4.76	5.01	5.15
				C.I.P.W. Normative Compositions.					
Q	—	—	—	—	—	—	—	—	—
or	7.21	8.45	9.33	7.15	7.68	9.80	11.11	7.09	7.27
ab	25.89	25.18	30.17	25.81	27.29	32.39	33.18	24.45	25.71
an	30.11	26.39	19.84	31.61	32.54	32.65	28.18	31.52	32.44
ne	—	1.21	1.01	—	0.21	—	0.27	0.69	0.42
di wo	8.15	9.47	9.89	8.06	6.11	3.99	7.05	8.02	8.22
en	4.86	4.39	3.88	4.37	3.12	1.64	3.22	4.04	4.05
fs	2.87	4.99	6.15	3.41	2.83	2.38	3.78	3.80	4.02
hy en	1.57	—	—	—	—	0.56	—	—	—
fs	0.93	—	—	—	—	0.82	—	—	—
Ol fo	7.06	7.19	5.26	7.99	7.72	2.60	1.77	8.36	6.69
fa	4.59	9.00	9.20	6.86	7.73	4.17	2.29	8.65	7.31
mt	3.99	0.65	0.51	2.32	2.25	6.79	5.77	0.74	1.32
il	2.20	2.66	2.93	2.16	2.20	2.87	3.08	2.15	2.20
ap	0.42	0.51	0.58	0.42	0.46	0.65	0.70	0.42	0.44

implication that the extents of amphibole stability fields defined here are upper limits. Helz (1982) suggests that increased total alkali contents may also expand the field of amphibole with respect to that of olivine or clinopyroxene leading to the possibility of increased involvement of amphibole in the evolution of more potassic are magmatic suites.

Amphibole compositions

The compositions of amphiboles synthesised is these experiments are given in Table 4 where Fe^{3+} values were estimated using the method of Spear and Kimbâll (1984). The Fe^{3+} values quoted in Table 4 are the average of the stoichiometrically-acceptable upper and lower ferric iron extremes. These are pargasitic hornblendes with Mg/(Mg + Fe) ratios in the range 0.58–0.75. They have very low SiO_2 and high Al_2O_3 contents and based on 23 oxygens have close to 6 Si atoms and 2 $Al^{(iv)}$ atoms per formula unit. They have Ti^{amph}/Ti^{liq} ratios of between 2 and 11 by weight, and $(K/Na)^{amph}/(K/Na)^{liq}$ values close to unity. Total K_2O and Na_2O contents are about 0.65 those of the coexisting melt.

In Table 4 the compositions of natural amphibole from Rindjani volcano are given for comparison. These include low pressure phenocrysts from dacites and presumed higher pressure phases present as reacted xenocrysts in andesite. By comparison with the xenocrysts the presumed lower pressure phenocrystic amphiboles have higher TiO_2 and SiO_2 and lower Al_2O_3 and CaO. The synthesised amphiboles are very like the natural xenocrystic group.

Liquid compositions

The recalculated liquid compositions for a number of runs are given in Table 3, together with their CIPW norms. It is noteworthy that only runs which contain amphibole show appreciable silica enrichment when compared to the initial high-Al basalt. Liquids from runs in the pyroxene, olivine and/or plagioclase fields have $< 51\%$ SiO_2. Similarly, the only runs whose liquids are *Q* normative are those which contain amphibole.

The compositions of the starting HAB (41632) and a typical Rindjani andesite (41625) are given in Table 1. The compositions of those experimental liquids whose compositions are confidently recalculated are plotted in Fig. 4 and 5. It is clear that in a broad sense the composition of liquids in equilibrium with amphibole are andesite-like (consider runs T150, T993, T994, T159, T1379 and T1383 in Table 3). They are quite silica-rich, aluminous and have calcalkaline character in terms of high $CaO/(K_2O$

Table 3. (continued)

T151*	T150*	T989	T153	T175	T993*	T994	T159*	T1377	T1384*	T1379*	T1383*
990	980	1120	1090	1065	1040	1030	1030	1040	1020	1000	950
5 atm	5 atm	10 atm	10 atm	10 atm	10 atm	9 atm	10 atm	10 atm	10 atm	10 atm	10 atm
5	5	5	5	5	5	5	5	5	5	5	5
50.93	55.26	49.76	49.77	49.74	54.40	54.41	55.27	49.62	51.68	56.23	58.52
1.17	0.50	1.13	1.14	1.26	0.32	0.32	0.26	1.21	0.84	0.34	0.19
19.67	19.13	17.87	18.12	20.08	18.74	18.65	18.04	19.31	18.15	18.50	20.48
2.30											
7.07	8.40	9.78	9.87	9.77	9.86	10.37	9.54	9.43	9.58	8.15	3.90
0.16	0.30	0.15	0.16	0.16	0.11	0.28	0.26	0.15	0.18	0.30	0.14
3.51	0.87	6.46	6.22	4.69	1.78	1.57	1.30	5.38	4.39	1.53	1.23
10.44	9.75	10.42	10.17	8.21	10.10	9.37	10.13	9.27	10.20	9.68	9.89
3.49	3.79	3.04	3.12	3.65	3.34	3.32	3.50	3.39	3.23	3.48	3.72
1.35	1.64	1.21	1.24	1.50	1.38	1.36	1.36	1.35	1.26	1.42	1.46
0.21	0.35	0.18	0.19	0.22	0.29	0.36	0.31	0.20	0.23	0.38	0.46
0.47	0.16	0.54	0.53	0.46	0.24	0.21	0.20	0.50	0.45	0.25	0.36
0.39	0.43	0.40	0.40	0.41	0.41	0.41	0.39	0.40	0.39	0.41	0.39
16.40	51.70	0.30	3.20	22.10	40.20	43.30	45.00	11.30	21.00	46.40	54.50
5.86	9.32	5.01	5.17	6.42	7.56	7.95	8.19	5.64	6.33	8.40	9.90
—	4.89	—	—	—	4.89	6.36	5.97	—	—	7.58	9.98
7.98	9.69	7.15	7.33	8.86	8.16	8.10	8.04	7.98	7.45	8.39	8.63
29.53	32.07	25.72	26.40	30.89	28.26	28.35	29.62	28.69	27.33	29.45	31.48
34.02	30.34	31.54	31.78	33.98	32.07	32.35	29.50	33.49	31.31	30.67	34.87
—	—	—	—	—	—	—	—	—	—	—	—
6.85	6.57	7.92	7.28	2.22	6.74	5.13	7.82	4.67	7.43	6.21	4.67
3.25	1.33	4.71	4.27	1.15	2.07	1.44	1.89	2.59	3.76	1.88	1.93
3.51	5.72	2.80	2.66	1.00	4.93	3.92	6.40	1.90	3.50	4.54	2.77
1.26	0.84	1.57	1.50	1.12	2.36	2.52	1.35	0.85	6.23	1.93	1.13
1.36	3.60	0.93	0.94	0.97	5.63	6.83	4.59	0.62	5.81	4.72	1.63
2.97	—	6.87	6.81	6.54	—	—	—	6.98	0.66	—	—
3.54	—	4.50	4.69	6.33	—	—	—	5.64	0.68	—	—
3.33	3.36	3.91	3.95	4.20	3.82	3.78	3.84	4.05	3.95	3.27	1.56
2.22	0.95	2.15	2.16	2.39	0.61	0.61	0.49	2.30	1.60	0.65	0.36
0.49	0.81	0.42	0.44	0.51	0.67	0.84	0.72	0.46	0.53	0.88	1.07

1. Liquid compositions are recalculated from microprobe analyses of quenched glasses using a mass balance technique (see text)
2. Where Fe^{3+} values are quoted, these are recalculated from total Fe as FeO consistent with olivine-liquid Kd value for MgO-FeO of 0.3
3. Analyses are normalised to 100% anhydrous
* Denotes runs containing amphibole

+ Na_2O) relative to silica content (Peacock 1931). However if detailed comparison is made between andesite 41625 (Table 1) and the liquids from well inside the amphibole field, it is clear that they differ in several important respects. In particular, the experimental liquids have lower MgO and much lower TiO_2 and somewhat higher CaO contents than the natural andesites. This is illustrated in Fig. 4 where experimental liquids are directly compared with the fields of natural Rindjani lavas (Foden 1983). From Fig. 4 it is clear that once cooled into the amphibole field, the liquids quickly evolve to compositions unlike those on the calc alkaline line of descent and that this deviation takes place from the amphibole-in reaction boundary (heavy arrow in Fig. 4).

The compositions of liquids in runs T993 and T175 at 10 kbar, and T151 and T150 at 5 kbar, straddle the low silica part of the Rindjani andesite field. This liquid is a basaltic andesite with about 53–54% SiO_2. This is an important observation as these compositions correspond to those of liquids which lie directly on the amphibole-out reaction boundary (Fig. 5). The water content of each melt was also calculated (Table 3). These calculations show that for instance, in run T993 which is just inside the amphibole field at 10 kbar and 1040°C, there are 40% crystals and the liquid contains 7.5 wt% H_2O.

Figure 5 shows liquids from 10 kbar runs plotted in the CMAS system in a projection from silica onto the CS-MS-A plane. The compositional fields of experimental clinopyroxene and amphibole are also shown. The range of Rindjani andesites and dacites is plotted and the position of the reaction boundary between the fields of clinopyroxenequid and that of amphibole + liquid is shown for this part of the system. The experimental liquid trend crosses the trend of the Rindjani suite at about 1030°C (at 10 kbar) and diverges away from the natural rock trend at lower temperatures. This temperature is directly on the amphibole reaction boundary where a restricted three phase (amph + cpx + L) field exists. "L" here refers to a liquid of the composition of low silica andesite.

We infer that the evolution of parental andesite by clinopyroxene (± olivine) separation takes liquids to basaltic andesite composition which corresponds to the amphibole/clinopyroxene reaction boundary. Further evolution to give the Rindjani-type calc alkaline trend to

Table 4. Electron microprobe analyses of synthesised and natural amphiboles

Run number	T151	T150	T1000	T994	T85	T1498	T993	T1384	T1379	T1383	T1495	41641	41645
Temperature °C	990	980	990	1030	1000	1000	1040	1020	1000	950	950	Dacite-	Andesite-
Pressure kbar	5	5	7.5	9	10	10	10	10	10	10	10	Pheno.	Xenocry.
Wt.% H_2O in Run	5	5	8	5	2	2	5	5	5	5	5		
SiO_2	42.55	42.68	41.69	40.81	41.81	40.65	40.78	41.66	40.04	41.64	41.59	42.52	40.59
TiO_2	2.55	1.70	1.81	2.53	2.81	4.25	2.38	2.22	2.28	2.11	2.12	3.11	2.09
Al_2O_3	15.28	15.96	15.49	15.94	16.13	14.70	15.84	16.35	16.50	15.12	15.46	10.32	13.18
FeO	8.55	10.73	9.24	9.51	13.01	14.17	9.78	9.18	11.07	14.38	13.15	13.15	12.99
MnO	0.00	0.00	0.00	0.00	0.00	0.15	0.20	0.00	0.00	0	0.24	0.33	0.13
MgO	13.91	11.72	13.91	13.92	11.38	10.17	13.77	14.32	12.73	10.93	11.60	13.43	14.83
CaO	11.54	10.77	11.05	11.12	9.66	10.44	10.67	11.22	10.59	10.41	10.64	10.75	12.44
Na_2O	1.83	2.20	2.24	2.50	2.53	2.24	2.46	2.24	2.39	2.27	2.28	2.85	2.51
K_2O	0.85	0.73	0.91	0.91	1.11	1.62	0.86	0.92	0.89	0.98	0.91	0.86	0.49
Cation totals based on 23 oxygens													
Si	6.150	6.241	6.081	5.925	6.042	6.004	5.940	5.961	5.877	6.108	6.065	6.302	5.848
Ti	0.280	0.187	0.199	0.276	0.305	0.472	0.261	0.239	0.252	0.233	0.233	0.347	0.225
Al (iv)	1.850	1.759	1.919	2.075	1.958	1.996	2.060	2.039	2.123	1.892	1.935	1.698	2.152
Al (vi)	0.750	0.993	0.745	0.654	0.790	0.563	0.660	0.719	0.733	0.723	0.723	0.106	0.087
Fe^{3+}	0.200	0.164	0.333	0.343	0.417	0.152	0.444	0.391	0.453	0.385	0.389	0.321	0.82
Fe^{2+}	0.840	1.148	0.795	0.812	1.155	1.598	0.748	0.708	0.906	1.379	1.215	1.309	0.745
Mn	0.000	0.000	0.000	0.000	0.000	0.019	0.025	0.000	0.000	0.000	0.030	0.041	0.016
Mg	3.000	2.554	3.024	3.012	2.451	2.239	2.989	3.054	2.785	2.389	2.521	2.967	3.185
Ca	1.790	1.688	1.727	1.730	1.496	1.652	1.665	1.720	1.666	1.636	1.663	1.787	1.921
Na	0.513	0.624	0.634	0.704	0.709	0.641	0.695	0.621	0.680	0.646	0.645	0.819	0.701
K	0.157	0.136	0.169	0.169	0.205	0.305	0.160	0.168	0.167	0.183	0.169	0.163	0.09
Na (M4)	0.158	0.266	0.179	0.173	0.386	0.305	0.209	0.169	0.206	0.255	0.228	0.202	0
Na (A)	0.354	0.358	0.455	0.531	0.323	0.337	0.485	0.452	0.474	0.391	0.417	0.617	0.701
Total A-site	0.511	0.494	0.624	0.699	0.527	0.642	0.645	0.620	0.640	0.574	0.586	0.78	0.791
$Fe^{3+}/Fe^{3+}+Fe^{2+}$	0.19	0.13	0.30	0.30	0.27	0.09	0.37	0.36	0.33	0.22	0.24	0.20	0.52
$Mg/Mg+Fe^{2+}$	0.78	0.69	0.79	0.79	0.68	0.58	0.80	0.81	0.75	0.63	0.68	0.69	0.81

Note: Analyses performed on a JEOL 733 Microprobe at University of Adelaide.
Recalculations are after the method of Spear and Kimball (1984)

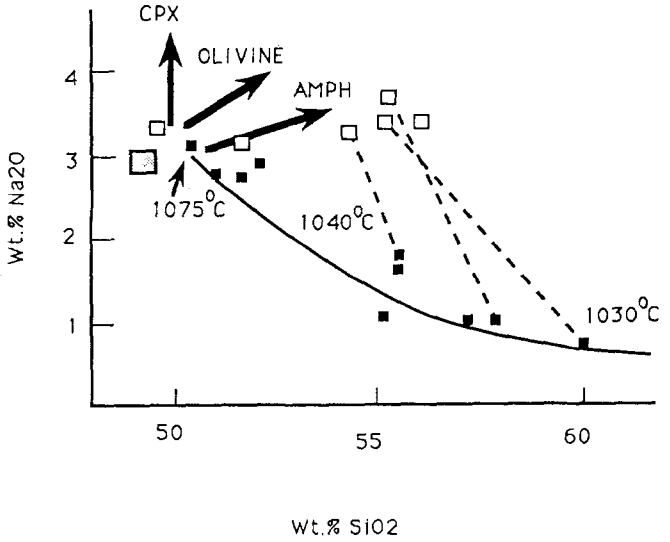

Fig. 3. Comparison between the *recalculated* (see Table 5) experimental melt compositions (*open squares*) and the electron microprobe analyses subject to Na loss, of the glasses (*filled squares*) for runs conducted at 10 kbar with 5% total water. Note that the run whose temperature is indicated as 1030 °C was 45% crystalline and the water content of the liquid 8% while that at 1040 °C was 40% crystalline and with 7.5% water dissolved in the melt. The *shaded square* is the starting composition and the *bold arrows* show the expected SiO_2–Na_2O covariation of the liquid due to crystallisation of the indicated phases

andesite and dacite is a lower pressure phenomenon, controlled by clinopyroxene and plagioclase (± orthopyroxene, ± magnetite) fractionation as well as by magma/phenocryst mixing.

Apparent trends in pseudoternary projection

Several recent studies adopt a strategy whereby natural whole rock compositions are projected in pseudoternary phase diagrams (e.g. Baker 1987; Baker and Eggler 1983). In some cases quite specific conditions of liquid equilibration are inferred on the basis of the similarity of the position of these data and experimental cotectics (liquid lines of multiple saturation). Our own study presented here allows examination of the rationale of such an approach and reveals several potential pitfalls. To be strictly comparable with the multiply saturated, experimental, univariant "trends", the natural rock data set should represent liquids which have the same multiple saturation as those used to establish the phase boundaries. Even though fractionating magmatic suites will produce curvilinear trends in these projections by precipitating only a single phenocryst, their positions will not solely reflect P, T and H_2O content, as these liquids are not buffered. Such trends would not be interpretable in the manner of Baker (1987) or Baker and Eggler (1983).

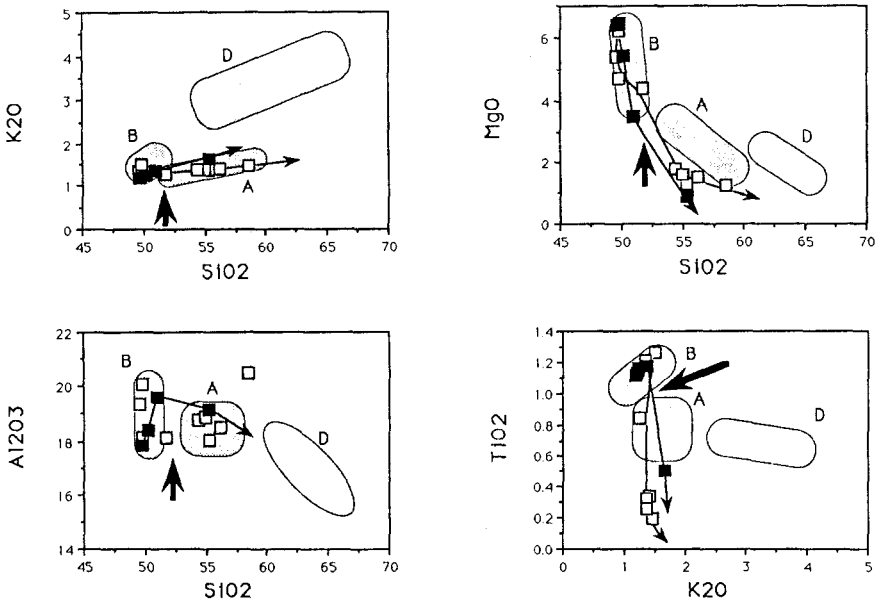

Fig. 4. The compositions of liquids from 5 to 10 kbar run series with 5% H_2O, plotted on variation diagrams showing the fields of the compositions of lavas from Rindjani volcano (Foden 1983). *B*, basalt; *A*, andesite; *D*, dacite. 5 kbar runs plotted (*filled squares*) are nos. T127, T131, T151, T150 and 10 kbar runs (open squares) are T989, T153, T175, T993, T159, T1377, T1384, T1379, T1383 (see Table 3). Note that some points are obscured. The *thin arrows* illustrate the trends of compositional variation of the experimental melts. The *thick arrows* show the point of appearance of amphibole on these trends.

Table 5. Example of the results of recalculation of analysed glass by least squares mixing to give estimated melt composition

	Start 41632	Cpx	Plag.	Olivine	Probe T71 Glass	Recalculated est. T71	Difference	
SiO_2	49.77	49.67	50.58	38.05	51.70	51.18	−0.52	
TiO_2	1.13	0.95	0.00	0.00	1.33	1.41	0.0	
Al_2O_3	17.84	7.59	30.62	0.00	19.68	20.07	0.39	
FeO	9.75	7.44	0.88	22.29	9.65	10.54	0.89	
MnO	0.15	0.16	0.00	0.30	0.13	0.16	0.02	
MgO	6.49	14.70	0.10	35.60	3.38	3.35	−0.03	
Cao	10.45	18.47	13.98	1.33	8.16	9.06	0.89	Σ
Na_2O	3.04	0.36	2.96	0.00	3.52	3.91	0.39	Difference
K_2O	1.20	0.00	0.26	0.00	1.80	1.69	−0.11	Squared = 2.19
P_2O_5	0.18	0.00	0.00	0.00	0.30	0.26	0.04	
	2% H_2O					2.85% H_2O		

Phase	Wt Fraction
Basalt	41632 1
Cpx71	−0.154
Plag71	−0.087
Olivine71	−0.053
Estimated Liquid 71	0.706

% Crystallisation = 29.42
% Residual Liquid = 70.6
% H_2O in Residual Melt = 2.85

Note: T71 refers to experimental run T71 and its products. Refers to Tables 2 and 3

This problem is illustrated when the compositions of liquids from some of our experimental runs (10 kbar with 5% H_2O) are plotted on the Plagioclase-Olivine-Silica + Orthoclase projection of Baker (1987) together with a representative selection of Rindjani lavas (Fig. 6). In this diagram, liquids from amphibole-bearing runs are indicated (and contain amphibole as the only solid phase). As already discussed, although the very siliceous liquids from these runs have compositions unlike real andesites, nevertheless on this projection they form a fairly convincing trend, overlapping some of the field of the Aleutians data (Atka) as shown in Fig. 6 (from Baker 1987). On the basis of the reasoning applied by Baker (1987) rocks of the compositions of these experimental liquids would erroneously be attributed to an origin at 0.5–2 kbar with 2–3% H_2O.

Discussion

The role of amphibole

An important immediate conclusion, contrary to the model proposed by Foden (1983), is that calcalkaline andesitic liquids do not evolve by direct *fractional* crystallisation of pargasitic amphibole from basaltic parent magmas. This mechanism would require that such liquids have amphibole on their liquidi at some pressure. Nevertheless the petrological literature contains numerous references to the occurrence of amphiboles (of the pargasite-hastingsite group) as xenocrysts, phenocrysts, or xenoliths in mafic island arc lavas (e.g. Kanaga Island, Alaska, Delong et al. 1975; Rindjani volcano, Indonesia, Foden 1983; Sangeang Api volcano, Indonesia, Foden and Varne 1983;

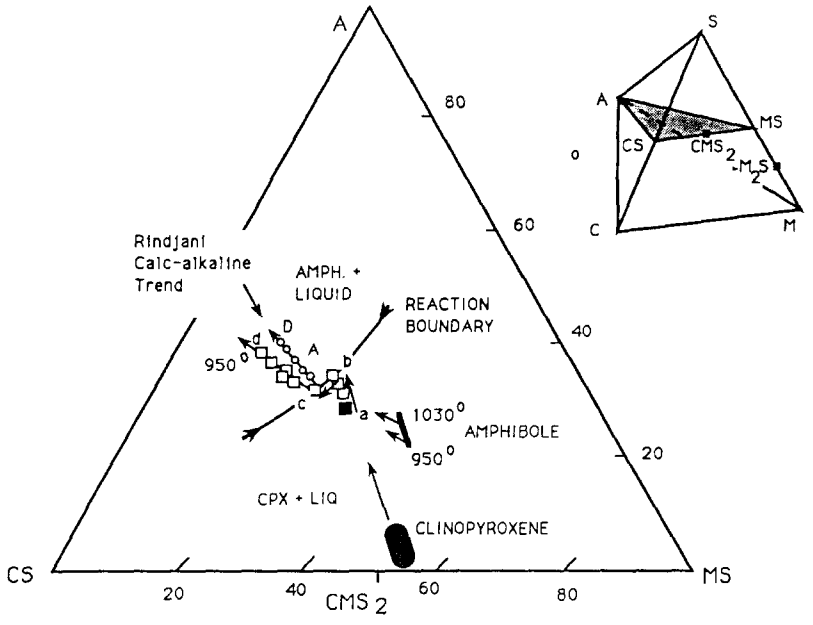

Fig. 5. The compositions of the same 10 kbar experimental liquids as plotted in Fig. 3, plotted in the system CMAS on the A-CS-MS section projected from silica. The *shaded square* is the starting basalt composition, 41632 (Table 1). The fields of synthesized clinopyroxenes and amphiboles are shown with arrows representing the direction of compositional control by these phases on the liquid; clinopyroxene control along segment a–b, buffering on the reaction boundary along segment b–c and amphibole control along segment c–d. The trend defined by circles represents the compositions of typical andesites (*A*) and dacites (*D*) from Rindjani volcano (Foden 1983). Also shown is the inferred position of the reaction boundary between the clinopyroxene + liquid and amphibole + liquid fields and its down-temperature directions

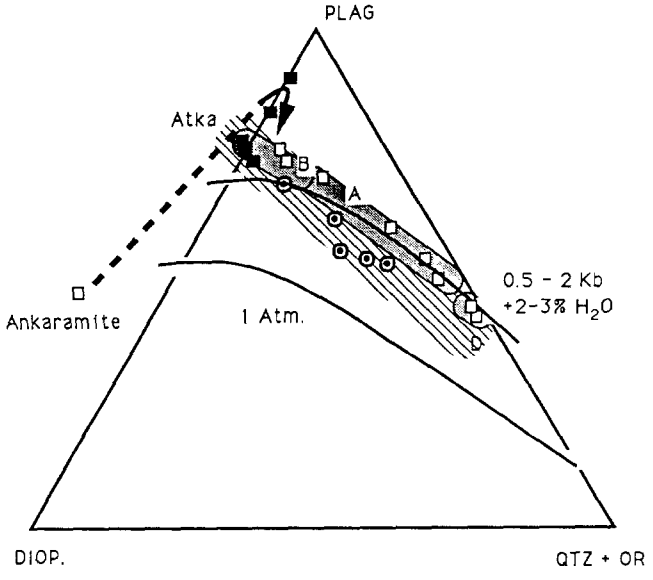

Fig. 6. A projection from magnetite of the Plagioclase-Diopside-Quartz + Orthoclase pseudoternary phase diagram of Baker and Eggler (1983) with their 1 Atm-dry and 0.5–2 kbar + 2–3% H_2O cotectics (multiple saturation of plagioclase-olivine ± clinopyroxene ± orthopyroxene). The *cross-hatched field* shown is that of the Aleutian Atka suite from Baker and Eggler (1983). *Encircled spots* are experimental liquids from this work at 10 kbar + 5% H_2O which were in equilibrium with amphibole, *filled squares* are liquids in equilibrium with clinopyroxene. The *large shaded square* is the starting high-Al basalt 41632. The *open squares* are the compositions of typical Rindjani lavas (*B*, high-Al basalt; *A*, andesite, *D*, dacite; Ankaramite is the typical composition of some rare highly olivine-clinopyroxene-phyric lavas also from Rindjani). The trend between the ankaramite and high-Al basalt is probably partly accumulative. The *arrow* indicates the complementary liquid evolution direction and the onset of plagioclase precipitation

Lesser Antilles, Lewis 1973; Arculus and Wills 1980; Japan, Aoki 1971; Aleutian Islands, Kay and Kay 1985, Debari et al. 1987, Conrad and Kay 1984). Murray (1972) and others (e.g. Foden and Varne 1983; Conrad and Kay 1984) have also suggested that Alaskan-type, zoned ultramafic complexes (e.g. Irvine 1974) which often include hornblende-rich assemblages, are the feeder zones of island arc volcanoes.

Amphibole may occur in magmatic systems of broadly basaltic composition if cooling and mineral growth is by closed system, *equilibrium* crystallisation. This mode of crystallisation is developed when the body of magma as a whole becomes stationary. Under these conditions vigorous convection and mixing will occur in the interior of the magma body and phenocrysts and melt will maintain equilibrium. The magma body as a whole will cool and the early formed phenocrysts of clinopyroxene and olivine will eventually enter a reaction relationship with the melt to produce amphibole. As our experimental results indicate, the reaction relationship between hydrous basaltic liquid and olivine or clinopyroxene exerts a mineralogical and thus chemical buffering constraint on the composition of the melt as long as the reactants and products are present. Under the conditions described in these experiments the buffered liquid is of basaltic andesite composition.

This amphibole-out reaction buffer will also operate in more open magmatic systems when the wall-rocks with which the cooling, hydrous basaltic melts are in contact are composed of olivine and pyroxene. This is of course the case in the upper mantle where in addition to mantle peridotite, fractionating primary basalts may also leave cumulate bodies of olivine clinopyroxenite. In many real situations there will be an oversupply of reactants and their conversion to amphibole will always be incomplete (Fig. 8a). Therefore as these liquids will not leave the reaction boundary (point C in Fig. 7) they will be buffered in the manner already described, to low silica andesite composition (basaltic andesite).

The reaction buffering model proposed here is supported by the common observation that when amphibole is present in olivine clinopyroxenite xenoliths in island arc rocks, it is forming at the expense of clinopyroxene and/or

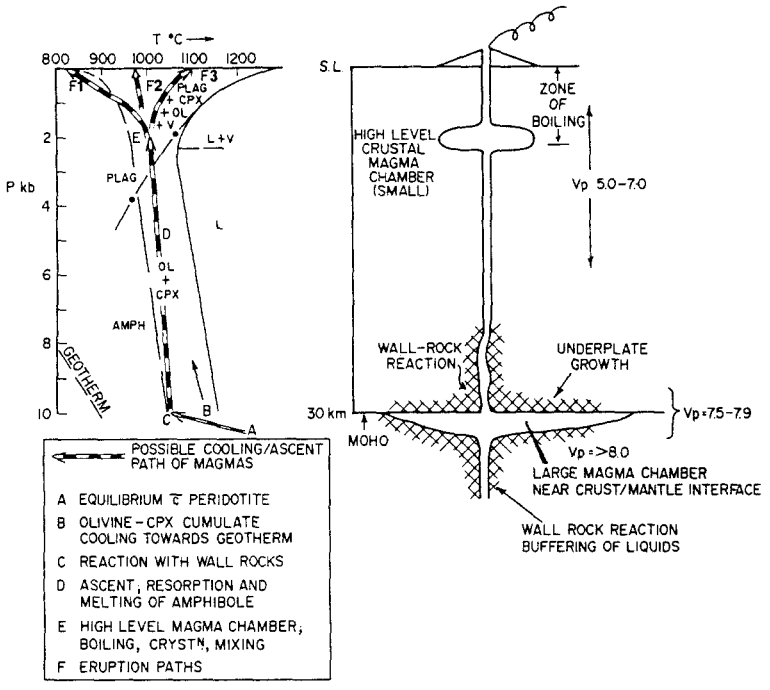

Fig. 7. A summary phase diagram (*left*) for the high-Al basalt system discussed in this paper with 5% H_2O showing possible cooling/ascent paths and the crystallisation products at each stage. The *right hand diagram* indicates a conceptual crustal section of an Indonesian-style (or Japanese, or Aleutian) island-arc

olivine (e.g. Conrad and Kay 1984). This is well illustrated by material from Sangeang Api volcano, Indonesia (Fig. 8a) and by the assertion that clinopyroxene-rich xenoliths from Adak, in the Aleutians show pargasitic "alteration" at between 980 and 1050°C (Debari et al. 1987).

The wall-rock buffering mechanism proposed here will be efficient if the melt and anhydrous ferromagnesian silicate phases are maintained in contact under broadly isobaric conditions. However if these liquids are tapped and extracted from the crystalline matrix or residues to rise into the crust (path D, Fig. 7), they will probably move directly back into the field of olivine and clinopyroxene (+ plagioclase). The adiabatic (constant entropy) temperature gradient of a magma is given by:

$$(dT/dz) = ga_fT/Cp$$

where g is the acceleration due to gravity, a_f the thermal expansion coefficient of the magma, T the absolute temperature, z the distance decompressed and Cp the specific heat at constant P. Substituting appropriate values (e.g. McKenzie 1984) this yields a melt temperature gradient of about -1 °C per km of decompression, significantly less than the gradient on the amphibole-out curve (Fig. 1) which is at least -3 °C/km at pressures less than 10 kbar. As a result, amphibole of this early (higher pressure) generation will seldom be observed entrained in erupted magma. Any such amphibole will tend to undergo decompressive incongruent melting and, as illustrated in Fig. 8b, will form xenocrysts with pyroxene-rich coronas. The incongruent melt produced in these circumstances will either be lost to the entraining magma leaving simple pyroxene-rich rims (Fig. 8d), or when larger polycrystalline amphibole-bearing xenoliths are involved these may retain the incongruently produced melt in the form of glass (Figs. 8c, e). The reactivity of these higher pressure phases complements the observation that the mineralogy of arc volcanic rocks is dominated by phases of crustal origin.

Polybaric crystallisation

There is good evidence that many calc alkaline suites are the composite products of several petrogenetic steps. Melt fractionation is polybaric and mixing of magma batches at different stages of evolution is a common phenomenon. The evidence for polybaric evolution is both geophysical and petrological.

High-Al basalt and andesite generally have large proportions of phenocrysts crystallised at low pressures. These are plagioclase, pyroxene and magnetite assemblages which are in equilibrium with groundmass mesostasis or glass of dacitic composition (e.g. Foden 1983; Crawford et al. 1987). As Foden (1983) pointed out, the relationship between andesite and dacite is one of nearly isothermal unmixing of phenocryst phases and it is probable that this process is governed by preferential liquid extraction from partly crystalline magmas in the relatively high-level crustal magma chambers supplying arc stratovolcanoes. By contrast the trends from basalt to andesite require the extraction of cumulates that are more silica deficient than the bulk composition of the low pressure phenocryst phases.

The polybaric origin of arc magmas is supported by geophysical studies. These studies commonly identify two broad groups of magma chambers beneath large strato volcanoes; a crustal group at 5 to 20 km depth and a grouping of larger chambers in the uppermost mantle at the crust-mantle boundary (e.g. Utnasin et al. 1975; Balesta et al. 1977; Balesta pers comm. 1985; with respect

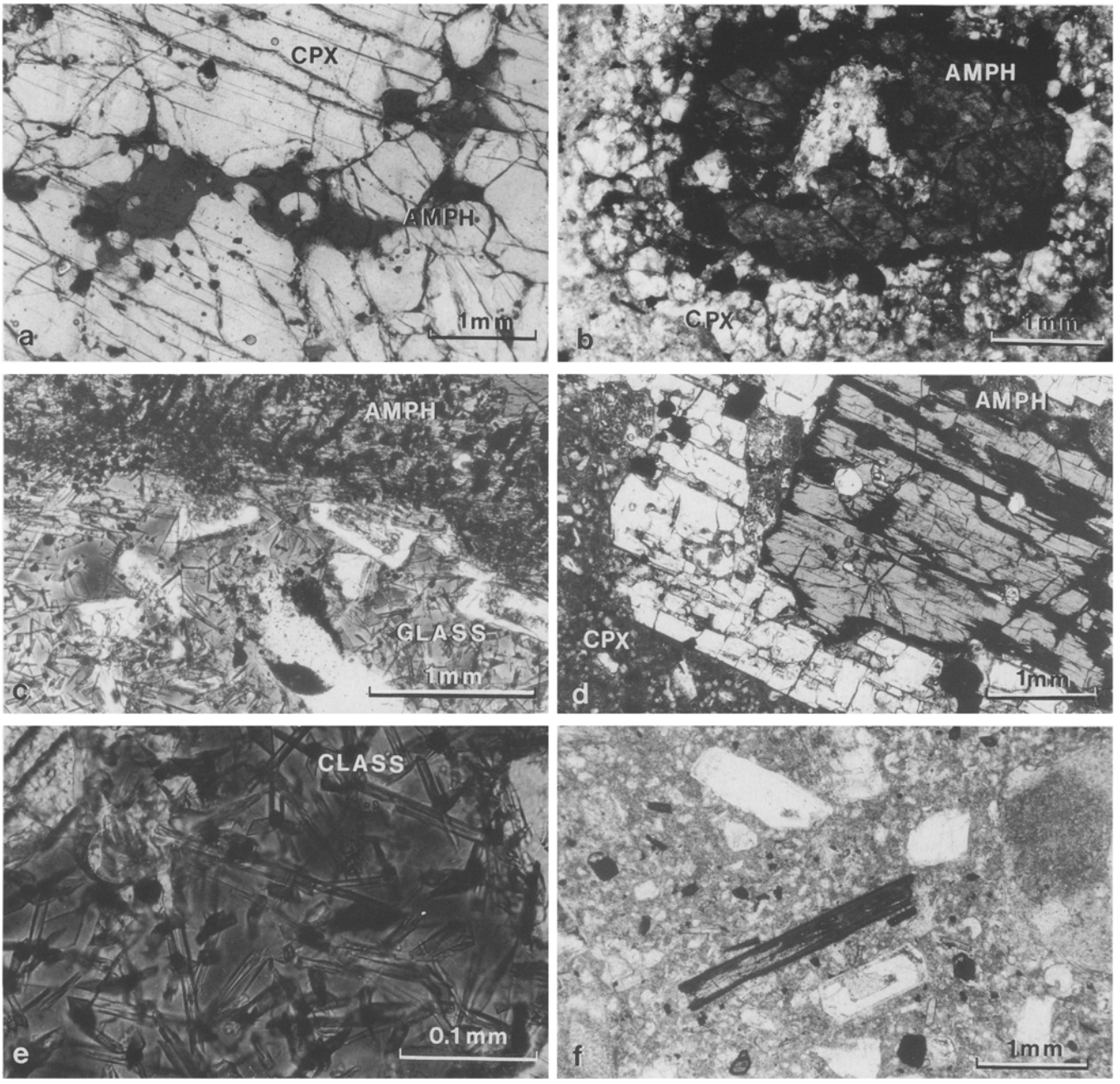

Fig. 8a–f. The most common types of petrographic association of amphibole in arc rocks are illustrated, and demonstrate the common occurrence of reaction and overgrowth relations. **a** Olivine-clinopyroxenite xenolith from Sangeang Api volcano, eastern Sunda Arc (Foden and Varne 1983). Originally of probable cumulate origin formed along path A–C in Fig. 7, pargasite is forming by reaction with a melt at a point (such as C in Fig. 7) to form clinopyroxene. CPX, clinopyroxene; AMPH, pargasite. **b** Pargasite (AMPH) xenocryst with a reaction corona of pyroxene and plagioclase entrained in an andesite lava flow from Kedang volcano on Lomblen Island, east Sunda Arc (Wheller et al. 1987). This is probably a decompressional melting reaction formed along path D, Fig. 7. **c** Partially melted pargasite (AMPH) from an amphibole gabbro xenolith from Sangeang Api volcano. The liquid (GLASS) was formed by this decompressive melting event along path D, in Fig. 7. **d** Pargasite (AMPH) xenocryst with a pyroxene (CPX) rim entrained in an andesite flow from Wai Sano volcano, Flores Island, east Sunda Arc. This may illustrate overgrowth of entrained amphibole during ascent along path D, Fig. 7. **e** An enlargement of the glass in Fig. 8c, produced by the decompressive partial melting of pargasite. This alkaline melt subsequently partially quenches to form the crystallites of olivine, spinel pyroxene and plagioclase contained in the glass. **f** The late overgrowth of amphibole (dark) on a pyroxene core formed during low pressure cooling back into the amphibole stability field (path E–F, Fig. 7)

to the Klyuchevskoy and Bezymianny volcanoes, Kamchatka). This crust-mantle interface region beneath arcs is also the common site of anomalous P-wave velocities with values between those of the crust and mantle (7.5–7.9 m/s) (Fig. 7).

Primary basaltic liquids and initial fractionation

As discussed by many authors, including Crawford et al. (1987), Ramsay et al. (1984), Kay and Kay (1985), Debari et al. (1987), Tatsumi et al. (1983), Murray (1972), and

Gust and Perfit (1987), there is good evidence that the parental magmas of island arc calcalkaline and tholeiitic suites are magnesian basaltic melts initially in equilibrium with peridotite. Following extraction from their asthenospheric source, the first stage of fractionation of these is controlled by olivine, clinopyroxene and spinel. The role of plagioclase at this stage is eliminated or inhibited by the presence of water (Figs. 2 and 6). Thus in Fig. 6 (Baker 1987) the displacement of the calc alkaline suite trends towards the plagioclase apex is a measure of the extent to which this "picrite/ankaramite" stage develops before aluminous phases (plagioclase at low pressure or amphibole at higher pressure) begin to crystallise. As illustrated on Fig. 6 this ankaramite control trend is probably in part accumulative. The crystallisation products of this early stage of arc magmatic evolution are seen as xenoliths (Fig. 8a) of olivine-clinopyroxenite, clinopyroxenite or dunite in some arc magmas (e.g. Conrad and Kay 1984; Foden and Varne 1983) and in Alaskan-type, zoned ultramafic complexes (Irvine 1974; Murray 1972). The magnesian parental melts are less commonly erupted but are nevertheless ocassionally recognised (e.g. Ramsay et al. 1984; Gust and Perfit 1987; Falloon and Green 1986). As Debari et al. (1987) and Kay and Kay (1985) point out, the cumulate products of the early stages of arc evolution constitute a petrological Moho and are commonly deformed and recrystallised. Their site of emplacement is dictated by their high density and likewise the parental melts themselves and probably do not rise readily through a crust which is not undergoing extension and thinning.

As illustrated in Figs. 7 and 2, this tendency to form ultramafic cumulates is not only dictated by water content, but also the pressure at which cooling takes place. Thus if the level of ponding is at higher pressures, as would be the case beneath arcs with thicker crust, then fractionation in the clinopyroxene-olivine field is favoured. When ponding levels are shallow, as may be the case in oceanic arcs with thin crust, fractionation within the plagioclase field is more likely.

Crystallisation at crustal pressures

The preceding discussion suggests that magmas which crystallise at uppermost mantle pressures beneath arcs with moderately thick crust will rise into the crust having fractionated clinopyroxene/ olivine, and may also have been modified by reactions which produce amphibole. These normative plagioclase-enriched, hydrous basaltic and basaltic-andesite melts will become water saturated and will be forced to crystallise plagioclase-dominated assemblages where the liquidus and the plagioclase-out curves change to negative dP/dT slopes (Fig. 7, point E). The residual liquids at this stage undergo rapid transition towards dacitic and rhyolitic compositions. The rheological and density changes in the magma that result from rapidly increased crystallinity and hydrous fluid exsolution will dictate the ponding level. Processes in these magma chambers, including magma mixing and vapour phase exsolution, generate the characteristic volcanological behaviour of calc alkaline magmas.

The cooling paths of ascending magmas may change to develop smaller dP/dT slopes than those of the amphibole-out curve which they may eventually re-cross (Fig. 7, path F1). In this case the commonly observed hornblende of siliceous andesite and dacite is developed. The fact that this stage of amphibole growth is quite late and from relatively cool and fractionated liquids is demonstrated by the overgrowth of amphibole on quite Fe-rich pyroxene (Fig. 8f).

In Fig. 7 two other final cooling paths (paths F2 & F3) are also indicated. The central one simply suggests that with continued adiabatic decompression and cooling, an ascending magma which at depth had been in equilibrium with amphibole may simply erupt with an anhydrous pyroxene-feldspar assemblage. The third indicated final eruption path entertains the possibility of late-stage heating. This would be a consequence of several factors including: (i) magma mixing, (ii) the entrainment of hotter mafic magmas by cooler felsic ones by draw-up during eruption of layered magma chambers, (iii) heating of overlying magma layers by rising high temperature vapour phases exsolved in lower layers (the espresso coffee machine model) and (iv) the release of latent heat of crystallisation during enforced decompressive precipitation of plagioclase.

Conclusions

The implications of the experimental data and discussion presented in this paper are that the characteristic of arc magmatism result mostly as a response to the unusual water content of arc magmas, coupled with locally unique thermal characteristics. In many ways, island arcs are not unlike lithospheric rifts of the "active" category (Keen 1985) with the important difference that the ascent of the asthenosphere in the central axial zone is not the result of the impingment of a deep-seated thermal plume. In the arc situation, a strip of asthenosphere becomes hydrated above the site of water-release in the down-going slab, resulting in viscosity reduction, diapirism and partial fusion. This ascends beneath the volcanic axis of the arc, thinning the lithospheric mantle in just the same manner as the active rift.

Because of the cold-finger effect of the down-going slab, the thermally anomalous upwelling beneath the volcanic axis is generated from what in reality is mantle with a potential temperature which is cool by comparison with "normal" asthenosphere. Vertical mobility of this peridotite and its partial melting are only possible because of the influence of water. In the McKenzie and Bickle (1988) parameterised model, anhydrous asthenosphere whose *potential temperature* is 1280 °C will produce basaltic melts by adiabatic decompression within 40 km or less of the surface. In the arc situation, melts are produced at lower temperatures. Because the solubility of water in magmas diminishes rapidly at pressures encountered in the crustal regime, rising hydrous melts must evolve by crystal fractionation so as ultimately to achieve compositions compatible with their temperature and, because of water loss, will approach anhydrous liquids at eruption.

Thus by comparison with other magmatic regimes, arcs are dominated by the solid crystallisation products of parental liquids and by the rocks formed from the resultant fractionated melts. In this paper we have particularly emphasised examples of these processes involving amphibole crystallisation, but would hasten to point out that as we are studying complex multi-variant systems, the scenarios we have elaborated are only one of several families of possibilities. Amongst these is the interesting possibility of localised incongruent partial melting of the postulated amphibole-enriched lower crustal regions to provide a possible source of some of the alkaline (shoshonitic) arc suites.

The end result of these processes is the relatively rapid production of a welt of thickened crust and uppermost mantle whose total composition is basaltic. This basaltic composition reflects a source lherzolite which is probably more refractory than MORB source together with addition of 'slab components' transferred by melt or fluid migration (Green 1976; Duncan and Green 1987). This will have a total bulk composition which only differs from MORB by virtue of the volumetrically minor addition of lithophile element rich fluids and melts from the downgoing slab. Continental crustal growth by accretion of these arc terrains will be significantly more mafic than existing average exposed continental crust and will contribute to a decrease in its average model age.

Acknowledgements. The experimental component of this work was undertaken at the University of Tasmania by JDF., partly whilst in receipt of a Commonwealth Postgraduate award and afterwards whilst the recipient of an Australian Research Council (ARC) award; both awards are gratefully acknowledged. DHG also acknowledges ARC support and we both thank Mr K. Harris who provided expert advice in the performance of the experiments. Dr R. Varne of the University of Tasmania provided many stimulating discussions of problems relating to arc petrogenesis.

References

Allen JC, Boettcher AL (1978) Amphiboles in andesite and basalt: II. Stability as a function of P-T-fO2. Am Mineral 63:1074–1087

Aoki K (1971) Petrology of mafic inclusions from Itinome-gata, Japan. Contrib Mineral Petrol 30:314–331

Arculus RJ, Wills K (1980) The petrology of plutonic blocks and inclusions from the Lesser Antilles arc. J Petrol 21:743–799

Baker D (1987) Depths and water content of magma chambers in the Aleutian and Mariana island arc. Geology 15:496–499

Baker DR, Eggler DH (1983) Fractionation paths of Atka (Aleutians) high-alumina basalts: Constraints from phase relations: J Volcanol Geotherm Res 18:387–404

Balesta ST, Farberov AI, Smirnov VS, Tarakanovsky AA, Zubin MI (1977) Deep crustal structure of the Kamchatkan volcanic regions. Bull Volcanol 40:260–266

Cawthorn GR (1976) Melting relations in part of the system $CaO–MgO–Al_2O_3–SiO_2–Na_2O–H_2O$ under 5 kb. pressure J Petrol 17:44–76

Cawthorn GR, O'Hara MJ (1976) Amphibole fractionation in calc alkaline magma genesis. Am J Sci 276:309–329

Conrad J, Kay R (1984) Ultramafic and mafic inclusions from Adak island: crystallisation history and implications for the nature of primary magmas and crustal evolution in the Aleutian arc. J Petrol 25:88–125

Crawford AJ, Falloon TJ, Eggins S (1987) The origin of island arc high-alumina basalts. Contrib Mineral Petrol 97:417–430

Dana Johnston A (1986) Anhydrous P-T phase relations of near-primary high-alumina basalt from the South Sandwich islands. Contrib Mineral Petrol 92:368–382

Debari S, Kay SM, Kay RW (1987) Ultramafic xenoliths from Adagdak volcano, Adak, Aleutian islands, Alaska: Deformed igneous cumulates from the Moho of an island arc. J Geol 95:329–341

Delong SE Hodges FN, Arculus RJ (1975) Ultramafic and mafic inclusions, Kanaga island, Alaska and occurrence of alkaline rocks in island arcs. J Geol 83:721–736

Duncan RA, Green DH (1987) The genesis of refractory melts in the formation of oceanic crust. Contrib Mineral Petrol 96:326–342

Eggler DH (1972) Amphibole stability in H_2O-undersaturated calcalkaline melts. Earth Planet Sci Lett 15:28–34

Eggler DH (1973) Principles of melting of hydrous phases in silicate melts. Carnegie Inst Washington Yearb 72:491–495

Falloon TJ, Green DH (1986) Glass inclusions in magnesian olivine phenocrysts from Tonga, evidence for highly refractory parental magmas in the Tongan arc. Earth Planet Sci Lett 81:95–103

Foden JD (1983) The petrology of the calcalkaline lavas of Rindjani volcano, East Sunda Arc: a model for island arc petrogenesis. J Petrol 24:98–130

Foden JD, Varne R (1980) The petrology and tectonic setting of Quaternary-Recent volcanic centres of Lombok and Sumbawa, Sunda Arc Chem Geol 30:201–226

Foden JD, Varne R (1983) Arc ankaramites, Sangeang Api xenoliths and cordilleran ultramafic to dioritic intrusive complexes: an updated concept of arc growth and development. Abst 6th Aust Geol Conven, Canberra 153–154

Gill JB (1981) Orogenic andesites and plate tectonics. Springer Berlin, Heidelberg, New York

Green DH (1976) Experimental testing of 'equilibrium' partial melting of peridotite under water-saturated, high-pressure conditions. Can Mineral 14:255–268

Green TH (1982) Anatexis of mafic crust and high pressure crystallisation of andesites. In: Thorpe RS (ed) Andesite: Orogenic andesites and related rocks. Wiley, Chichester, pp 465–487

Gust DA, Perfit MR (1987) Phase relations of a high-Mg basalt from the Aleutian island arc: implications for primary island arc basalts and high-Al basalts. Contrib Mineral Petrol 97:7–18

Helz RT (1982) Phase relationships and compositions of amphiboles produced in studies of the melting behaviour of rocks. In: Veblen DR, Ribbe PH (eds) Amphiboles: petrology and experimental phase relations. Reviews in Mineralogy, Vol. 9B. Mineralogical Society of America, Washington DC, pp 279–346.

Holloway JR (1973) The system pargasite $H_2O–CO_2$: a model for melting of a hydrous mineral with a mixed-volatile fluid. I. Experimental results to 8 kb Geochem Cosmochim Acta 37:651–666

Holloway JR, Burnham CW (1972) Melting relations of basalt with equilibrium water pressure less than total pressure. J Petrol 13:1–29

Irvine TN (1974) Petrology of Duke Island ultramafic complex, south eastern Alaska. Mem Geol Soc Am 138

Kay SM, Kay RW (1985) Role of crustal cumulates and the oceanic crust in the formation of the lower crust of the Aleutian arc. Geology 13:461–464

Keen CE (1985) The dynamics of rifting: deformation of the lithosphere by active and passive driving forces. Geophys J R Astron Soc 80:95–120

Kushiro I 1(972) Effect of water on the composition of magmas formed at high pressures. J Petrol 13:311–334

Lewis JF (1973) Petrology of ejected plutonic blocs of the Soufriere volcano, St. Vincent, West Indies. J Petrol 14, 81–112

McKenzie D (1984) The generation and compaction of partially molten rock J Petrol 25:713–765

McKenzie D, Bickle MJ (1988) The volume and composition of melt generated by extension of the lithosphere. J Petrol 29:625–679

Murray CG (1972) Zoned ultramafic complexes of the Alaskan type: Feeder pipes of andesitic volcanoes. Mem Geol Soc Am. 132:313–335

Nicholls IA (1974) Liquids in equilibrium with peridotitic mineral assemblages at high water pressures. Contrib Mineral Petrol 45:289–316

Nicholls IA, Ringwood AE (1973) Effects of water on olivine stability in tholeiite and the production of silica-saturated magmas in the island arc environment. J Geol 81:285–300

Peacock MA (1931) Classification of igneous rock series. J Geol 39:54–67

Ramsay WRH, Crawford AJ, Foden JD (1984) Field setting, mineralogy, chemistry and genesis of arc picrites, New Georgia, Solomon Islands. Contrib Mineral Petrol 88:386–402

Ringwood AE (1974) The petrological evolution of island arc systems. J Geol Soc London 130:183–204

Spear FS, Kimball KL (1984) RECAMP-a FORTRAN IV program for estimating Fe^{3+} contents of amphiboles. *Computers of Geoscience* 10:317–325

Tatsumi Y, Sakuyama M, Fukuyama H, Kushiro I (1983) Generation of arc basalt magmas and thermal structure of the mantle wedge in subduction zones. J Geophys Res 88:5815–5825

Taylor SR, McLennan SM 1985 The continental crust: its composition and evolution. Blackwell, Oxford

Utnasin VK Abdurakhimov AL, Anasov GI, Balesta ST, Budyanskiy Yu A, Markhinin Ye K, Fedorenko VI (1975) Deep structure of Klyuchevskoy group volcanoes and problem of magmatic hearths. Int Geol Rev 17:791–806

Varne R, Foden J (1986) Geochemical and isotopic systematics of eastern Sunda arc volcanics: Implications for mantle sources and mantle mixing processes. In: Wezel F-C (ed) The Origin of Arcs. Elsevier, Amsterdam, pp 159–189

Wheller GE, Varne R, Foden JD, Abbott MJ (1987) Geochemistry of Quaternary volcanism in the Sunda-Banda arc, Indonesia, and three-component genesis of island-arc basaltic magmas, J Volcanol Geotherm Res 32:137–160

Yoder HS, Tilley CE (1962) Origin of basalt magmas: an experimental study of natural and synthetic rock systems. J Petrol 3:342–532

Editorial responsibility: R. Binns